Article

Preparation and Performance of Cement-Stabilized Base External Curing Agent in a Desert Environment

Chenhao Wei [1], Zewen He [2,*], Jiachen Ma [1], Xiaohui Sun [3], Yana Shi [1], Qiang Yi [1] and Maoqing Li [1,*]

[1] Shaanxi Coal Chemical Industry Technology Research Institute Co., Ltd., Xi'an 710100, China; weich_edu@163.com (C.W.)

[2] School of Materials Science and Engineering, Chang'an University, Xi'an 710018, China

[3] CCCC SHEC Construction Technology Branch Company, Wuhan 430040, China

* Correspondence: hezewen@chd.edu.cn (Z.H.); maoqingl2024@163.com (M.L.)

Abstract: To explore and deal with the difficulty in curing cement-stabilized bases in desert environments, curing agents were prepared to enhance the curing effect on the base in this research. The composite curing agent was prepared through orthogonal experiments and the durability of the curing agent coating were studied by simulating a desert environment. Subsequently, the curing effect on the performance of bases was analyzed. Finally, the hydration degree of cement was studied via scanning electron microscope (SEM), thermogravimetric analysis (TG), and X-ray diffraction analysis (XRD), and the curing mechanism of the curing agent was explored. The results show that the composite (paraffin emulsion is the main component of the film, vinyl acetate-ethylene copolymer dosage is 20%, ethanol ester-12 dosage is 10%, and sodium silicate dosage is 18%) could effectively improve the water-retention performance (water-loss ratio: 2.36%) and mechanical properties of the specimen (7 d compressive strength: 7.48 MPa; 7 d indirect tensile strength: 0.70 MPa). The dry shrinkage coefficient of the specimen with composite curing agent was reduced by 116.26% at 28 days. The compressive strength of dry and wet freeze could reach 7.48 MPa and 6.88 MPa, respectively. The durability of the curing agent-coated base met the requirements of pavement performance in desert areas. The results of XRD, TG, and SEM indicated that the curing agent promoted hydration. In addition, the number of C-S-H gel and AFt crystals significantly increased. The curing difficulty of road bases in desert areas could be reduced effectively through the application presented in this study, which contributes to the conservation of natural and human resources.

Keywords: desert environment; curing agent; cement-stabilized base; road performance; curing mechanism

1. Introduction

Cement-stabilized base (CSB) material has been applied in most parts of China due to its good performance and low cost [1–3]. With the increase in highway-construction areas in China, more and more projects are in a severe desert environment. However, cement-stabilized bases are difficult to effectively hydrate at high temperatures. In addition, rapid loss of water easily leads to the cracking of the base structure, resulting in degradation of the cement-stabilized gravel base. Therefore, how to propose suitable curing methods for bases in desert areas to ensure strength and durability is significant for pavement construction in high-temperature and dry areas.

Some scholars [4–6] enhanced the strength of cement-stabilized gravel by adding fiber, rubber, and mineral filler. Sun [7] replaced part of the fine aggregate with rubber powder of the same particle size and found the shrinkage resistance of the base was enhanced. However, these additives have a poor effect on its strength. To make cement-stabilized base obtain high strength, Liu et al. [8] studied the effect of polyester fiber (PET) dosage on the water-loss rate and performance of cement-stabilized gravel. They found that the addition of PET changed the elastoplastic behavior of CSM. M. Olgun [9] also used polymer

fiber to enhance the compressive strength. Although fibers can form a staggered mesh structure and improve cement-stabilized gravel's durability, it is still difficult to disperse evenly in gravel during construction. Hoy et al. [10,11] researched the application of natural rubber latex on concrete aggregate and believed that NRL had a positive effect on the cyclic performance. Also, NRL could prolong the service life of cement materials [12,13].

The curing method significantly impacts the strength and durability of cement-stabilized materials [14,15]. Deng et al. [14] analyzed the mechanical properties of cement-stabilized gravel, learning that the strength of the mixture gradually increased with the extension of the curing age, and the strength tended to be flat after 28 days. He et al. [16,17] studied the relationship between the erosion resistance of cement-stabilized gravel and the curing age, and it was found that the erosion resistance of cement-stabilized gravel reached a stable state after 14 days of curing age. Mao [18] designed an insulated bag dedicated to the maintenance of bases, and compared it with the development law of the strength of bases under different curing environments. It is reported that the health preservation of the insulation bag could improve early strength, reaching 100% of the strength of the standard health particle.

However, water resources are scarce in desert areas, making it difficult to maintain bases with a large amount of water. If the base can be maintained with a curing agent instead of water spraying and covering curing, it will bring huge economic benefits to the project. According to the different characteristics of use, curing agents are divided into external curing agents and internal curing agents [19]. The curing agent was first used in concrete curing [20–25]. Xue et al. [26] selected different curing materials to study the effects of curing materials on the microstructure of cement concrete. The results showed that the crystallization particles of ettringite (AFt) in the composite curing agent specimens were rod-shaped and had a large particle size, indicating that the composite curing agent promoted cement hydration and formed a dense and uniform microstructure. D. Snoeck [22] used calcium alginate and gelatin as external curing methods, and the results showed that calcium alginate and gelatin could prevent cracking and delay the damage of capillary pressure to specimens. A.S. Al-Gahtani [20] compared the effects of different curing methods on concrete performance and found that the performance of acrylic-based curing agents was excellent.

At present, cement curing agents are mainly used for mortar and concrete [24,25,27–30], and there are few studies on the curing of cement-stabilized gravel in desert environments. The air humidity in desert areas is generally 3% to 15%, and the average annual rainfall in most areas is less than 50 mL, resulting in drought throughout the year. In summer, the daytime temperature is as high as 60 °C, and the night temperature can reach below 0 °C. In winter, the weather is cold and dry, and the temperature can reach below -30 °C [31–33]. The desert climate poses a severe challenge to the construction and maintenance of roads in desert areas [32,33]. However, there is insufficient research on the application of internal curing agents in extreme desert environments; with internal curing agents, it is easy to cause expansion and deformation of cement-based materials, resulting in a decrease in base density and destruction of internal pore structure [34].

Above all, to deal with the problems of rapid internal moisture evaporation and insufficient durability of road bases in deserts, curing agents with excellent performance through orthogonal experiments were prepared to maintain cement-stabilized bases, and their influence on the strength and durability of bases was studied. Subsequently, through the test of mechanical properties, the effect and curing mechanism of curing agent on the performance of cement-stabilized base were explored combined with SEM, TG, and XRD. Through this study, the curing problem of the road base in the desert area can be solved, and the durability of road bases can be improved.

2. Materials and Methods

2.1. Materials

2.1.1. Film-Forming Emulsions and Additives

In this paper, paraffin emulsion, styrene acrylic emulsion, vinyl acetate-ethylene copolymer (VAE) emulsion, and styrene-butadiene-styrene block copolymer (SBS) emulsions were mainly selected. The film-forming properties of each emulsion are shown in Table 1. Admixtures include the film-forming additive alcohol ester-12, the emulsifier OP-10, and the reinforcing agent sodium silicate. Alcohol ester-12, emulsifier OP-10, and sodium silicate are chemically pure.

Table 1. Film-forming performance indexes of emulsions.

Technical Indicators	Paraffin Emulsion	Styrene Acrylic Emulsion	VA Emulsion	SB Semulsion
Drying time (h)	2.1	1.5	1.5	1
Solubility	Insoluble	Insoluble	Insoluble	Insoluble
Film-forming heat resistance	Qualified	Qualified	Qualified	Qualified
Impact resistance	Wrinkles	Cracks	No cracks	No cracks
Film-forming state	Thick, softer film	Thin, elastic	Thin, transparent, smooth	Thin, transparent, smooth, elastic

2.1.2. Raw Materials for Cement-Stabilized Base

The cement is Jidong brand P.O42.5 silicate cement; the indexes and chemical compositions are shown in Tables 2 and 3. The aggregate gradations are shown in Table 4. The sand used is the mechanism sand according to the standard regulations (ISO).

Table 2. Technical properties of cement.

Indicator		Specification Requirements	Measured Value	Standard
Fineness (%)		≤10	5.4	GB175-2007 [35]
Water consumption of standard consistency (%)		/	28.9	
Stability (Ray's method) (mm)		≤5	1.1	
Setting time	Initial setting time (min)	≥450	482	JTGE30-2005 [36]
	Final setting time(min)	≤600	560	

Table 3. Compositions of cement, wt%.

Composition	CaO	Al_2O_3	SO_3	SiO_2	Fe_2O_3	MgO	TiO_2	LOI
Content	51.30	8.60	2.50	27.23	4.30	3.35	0.87	1.85

Table 4. Aggregate gradation of cement-stabilized base.

Size (mm)	19.00	16.00	13.20	9.50	4.75	2.36	1.18	0.60	0.30	0.15	0.08
Upper gradation limit (%)	100.00	93.00	86.00	72.00	45.00	31.00	22.00	15.00	10.00	7.00	5.00
Lower gradation limit (%)	100.00	88.00	76.00	59.00	35.00	22.00	13.00	8.00	5.00	3.00	2.00
Median gradation (%)	100.00	90.50	81.00	65.50	40.00	26.50	17.50	11.50	7.50	5.00	3.50
Synthetic gradation (%)	100.00	92.87	76.53	67.70	36.87	23.37	18.09	13.56	9.26	6.35	3.95

2.2. Sample Preparation

2.2.1. Preparation of Curing Agent Emulsion

The film-forming additive alcohol ester-12, emulsifier OP-10 (10% of the solid content of paraffin emulsion), and sodium silicate were mixed and stirred in deionized water with

a magnetic stirrer (30 min, 400 r/min) to obtain a well-mixed aqueous solution of additives. Secondly, the emulsion to be selected was stirred at a rotational speed of 400 r/min, and the aqueous solution of additives was slowly poured into the emulsion. Then, the aqueous solution was fully added, mixed, and stirred for 20 min to make it uniformly dispersed. Finally, paraffin wax emulsion was added to the emulsion, mixing and stirring for 30 min completely.

2.2.2. Preparation of Composite Curing Agent Emulsion

Based on the performance test of a single emulsion, the orthogonal test method was used to optimize the optimal ratio of each component. Additionally, the compound was further carried out to prepare the composite curing agent emulsion and used for the subsequent test of the performance of the specimen.

2.2.3. Preparation and Curing Conditions of Cement-Stabilized Base

The specimens used in the cement-stabilized crushed stone semi-rigid base mechanical test were all formed via the static pressure method. A 150 mm × 150 mm mold was used in this test for compressive strength, with indirect tensile strength and a modulus test. The sample was static pressed, keeping the pressure for 2 min. After forming, it needed to stand for 2–4 h and then demolding took place.

In this study, high temperature dry curing was used to simulate a desert environment. The humidity of desert environments can be 10%, and the surface temperature in summer can reach 60 °C [33]; the conservation conditions of this study are shown in Table 5.

Table 5. Curing methods of cement-stabilized base.

Maintenance Method	Environmental	Conditions
High-temperature drying curing (desert environment)	Cement-stabilized gravel specimens coated with different curing agents and uncoated curing agents were placed in a blast drying oven to simulate a desert environment	60 ± 2 °C, RH = 10%
Standard curing	Constant temperature and humidity curing room	20 ± 2 °C, RH = ≥95%
High temperature and wet curing	Cement-stabilized gravel specimens coated with different curing agents and uncoated curing agents were bagged and sprinkled with water in the bag and placed in an oven to simulate a high-temperature wet-curing environment	60 ± 2 °C, RH = ≥95%
Naturally curing	Indoor	Indoor temperature

2.3. Test Methods

2.3.1. Performance of Curing Agent Emulsion

(1)   Anti-ultraviolet aging performance of curing agent

In this paper, an ultraviolet aging test chamber was used to simulate the natural aging of thin films. The tinplate coated with curing agent was put into the ultraviolet aging chamber to simulate the ultraviolet aging test, and 6 ultraviolet lamps (UVB-313EL, 290–315 nm) were used as the ultraviolet light source to accelerate the ultraviolet aging test. The lamp tube was 30 cm away from the coating sample, the temperature was 38 ± 3 °C, and the surface condition of the coating after 400 h ultraviolet lamp irradiation was observed, and a gloss meter and spectrophotometer were used to observe the test plate before and after aging.

(2)   Adhesion properties of conditioner emulsions

Different curing agents were sprayed on the non-asbestos fiber cement pressurized board, and the adhesion strength of the film at three different positions was determined by using the PosiTest AT–A digital pull-out adhesion tester (DEFELSKO, Ogdensburg, NY, USA), standing in a ventilated place for 48 h until it was completely dried and had a certain bond strength (Figure 1).

Figure 1. Schematic diagram of the film pull-out test of the curing agent.

(3)   Water-retention properties of conditioner emulsions

Based on ASTM C309-03 and JT T522-2004, a mortar test was used as the performance test of the curing agent, and the water-retention performance of the mortar was evaluated via the 3 d water-loss rate combined with the performance-evaluation methods at home and abroad.

2.3.2. The Mechanical Properties of the Cement-Stabilized Base

(1)   Unconfined compressive strength

The strength at four different ages of 3 d, 7 d, 28 d, and 90 d was determined via the specification JTG E51-2009 [37].

(2)   Indirect tensile strength

Based on JTG E51-2009, the cured specimen was placed on the bead (width 18.75 mm, arc radius 75 mm), and another bead was placed directly above the specimen so that the specimen was closely combined with the bead and was at the top. Finally, it was pressurized at 1 mm/min, and the maximum pressure loaded after the specimen was destroyed was recorded.

2.3.3. Durability of Cement-Stabilized Base

(1)   Dry shrinkage performance test

Middle beam specimens with the dimensions 100 mm $\times$ 100 mm $\times$ 400 mm were used in this test, with press static pressure forming specimens. After the molding was completed, they were placed for one day, and then molded; the dry shrinkage performance of standard curing and specimens was measured at 20 °C $\pm$ 5 °C, RH 60% $\pm$ 5%.

(2)   Frost-resistance test

In this paper, it was decided to use the dry freezing method and wet freezing method to test the frost resistance of the cured specimens. According to JTG E51-2009, the ratio of the compressive strength with several freeze–thaw cycles in 28 days to the compressive strength without freeze–thaw cycles can be used to evaluate frost resistance.

2.3.4. Microscopic Detection and Analysis

(1)   XRD analysis

The phase composition of the hydration products was analyzed via an X-ray diffractometer (Bruker D8 ADVANCE, Rheinstetten, Germany). The cement slurry samples were in ethanol for 24 h to avoid hydration. The test angle range was 15°–70°, and the copper target was Kα radiation.

(2)   TG test

In this paper, the DSC-TGA (SDT650) thermal analyzer of TA company was used to evaluate the hydration degree of different cured cements for 3 d and 7 d, and the cement sample was taken about 2 mm under the curing agent film. The cement sample was loaded into 90 mL of alumina, and the heating process of the sample was protected via N2 gas from indoor temperatures up to 1000 °C.

(3)   SEM analysis

A scanning electron microscope (Hitachi S-4800) was used to scan the microstructures of the curing agent and the cement. The properties of the curing agent film were analyzed.

3. Results and Discussion

3.1. Performance Test Results of One-Component Curing Agent Emulsion

3.1.1. Anti-Ultraviolet Aging Performance of the Curing Agent

During the test, it was found that the gloss value of the SBS film reached 200 Gu, which was beyond the measurement range. Therefore, only the gloss of paraffin, styrene acrylic, and VAE films was measured, and the paraffin films gradually cracked after long-term ultraviolet irradiation. The morphology of the films is shown in Figure 2.

(**a**) Paraffin film   (**b**) Styrene acrylic film   (**c**)VAE film
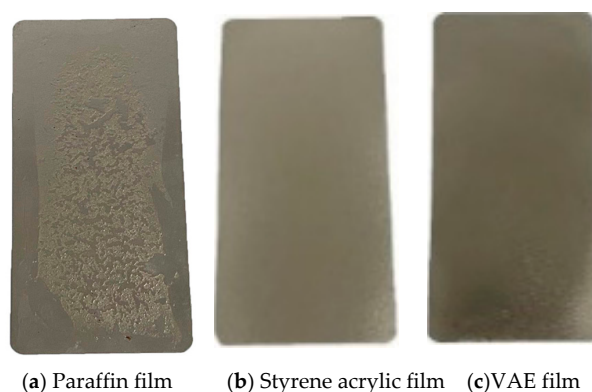
Figure 2. Different film appearances under UV irradiation.

The gloss of paraffin wax increases with aging time because the film gradually cracked over time and more areas of the tinplate were exposed to air, leading to an increase in gloss value. As shown in Figure 3, after 400 h of ultraviolet irradiation, the gloss value of styrene acrylic film and VAE film gradually decreased, and the gloss value of styrene acrylic film changed greatly, reaching about 25 Gu, while the gloss change value of VAE film was less than 10 Gu. The test results showed that the anti-ultraviolet aging performance of VAE film was stronger than that of paraffin film and styrene acrylic film.

As shown in Figure 4, after 400 h of UV aging, the paraffin film has the largest color difference (ΔE = 1.8), while the VAE and paraffin-VAE films have the smallest color difference (ΔE = 0.2). There is little difference between the color difference between VAE and paraffin-VAE films, indicating that the films formed via mixing VAE emulsions into paraffin emulsions had good anti-ultraviolet aging performance, which may be due to the uniform distribution of VAE emulsions with linear structure in paraffin emulsions.
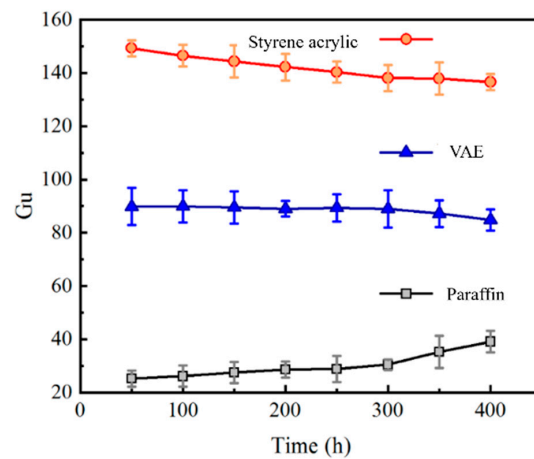
Figure 3. The effect of ultraviolet light on the gloss of different films.
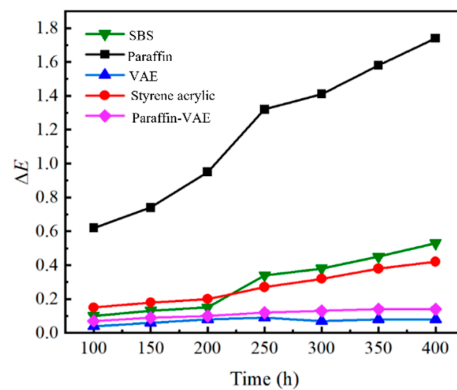
Figure 4. Chromatic aberration changes of different curing agent films during ultraviolet aging.

3.1.2. Adhesion between Curing Agent Emulsion and Cementitious Materials

In the construction process, the curing agent needs to be sprayed on the base surface. The pull-out test results show that the curing agent film and the cement board had good bonding properties. As shown in Figure 5, the pull-out strength of SBS, VAE, and styrene acrylic film and cement board is over 8 MPa, and the bonding strength of paraffin film and the cement board is the lowest. When VAE emulsion was mixed with paraffin emulsion, the pull-out strength of VAE emulsion was over 8 MPa, indicating that VAE emulsion and paraffin emulsion are more miscible. Therefore, the addition of VAE emulsion changes the bond property between paraffin film and cement board.
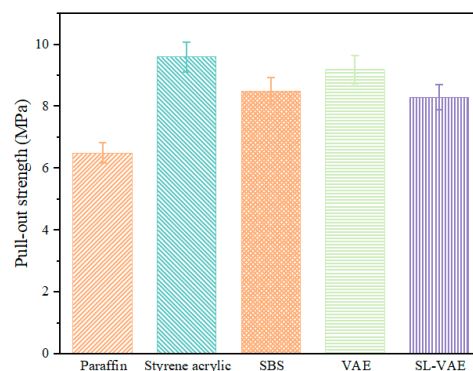
Figure 5. Different pull-out strengths between film and cement boards.

3.1.3. Water-Retention Properties of Conditioner Emulsions

Due to the poor film-forming properties of styrene-acrylic emulsions, the water-loss properties of paraffin emulsions, SBS emulsions, and VAE emulsions were tested. Water-loss rate of the curing specimen of the single curing agent is shown in Figure 6. It can be learned that the increased rate of water loss of the specimen gradually decreases as time goes by. The water-loss rate of the specimen coated with a curing agent and that without a curing agent was related to the type of curing agent. The 3 d rate of the uncoated curing agent specimen (control group) reached 88.05% of that at 7 d. In addition, the 3 d/7 d water-loss ratio of the curing agent group reached about 0.7, while the 3 d water-loss rate of the control group was 2.57 times that of the paraffin curing group. It was indicated that the water-retention performance of the blank group was the worst, and the water-retention effect was followed by the VAE curing CSB and the SBS curing CSB.
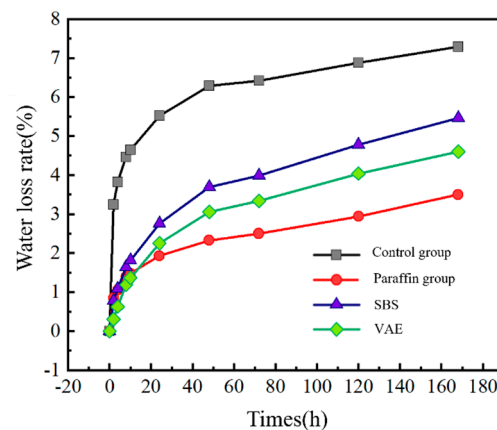

Figure 6. Water-loss rate of cement mortar.

The relationship between the content of VAE emulsion and the 3 d water-loss rate of the mortar is shown in Figure 7. Sodium silicate was added to the paraffin emulsion to explore the relationship between the sodium silicate content and the 7 d strength of the mortar (Figure 8). Before the VAE emulsion content reaches 50%, the water-loss rate is in the range of 20–30%. Additionally, the optimal dosage of VAE emulsion makes the water-loss rate of the mortar the lowest. Since the appropriate dosage of VAE emulsion could enhance the film-forming curing effect of paraffin curing agent on mortar, and the miscibility of VAE emulsion and paraffin emulsion was poor, the water-holding performance of the film formation was reduced. When the sodium silicate content was more than about 15%, the strength tended to be stable. SiO_3^{2-} in the emulsion met the normal needs of cement hydration, and too much sodium silicate increased the viscosity of the emulsion, which was not conducive to the spraying and brushing of curing agents.
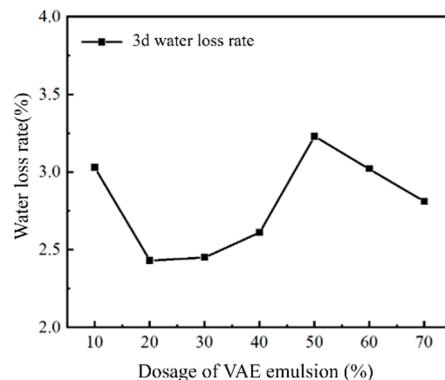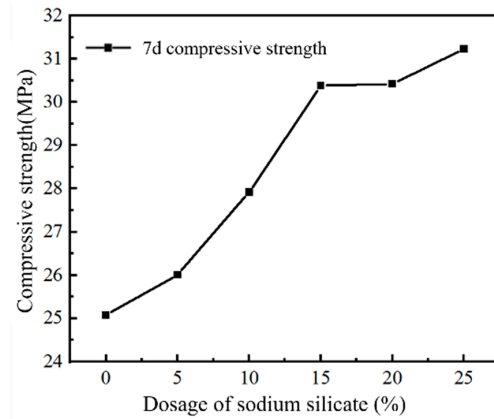

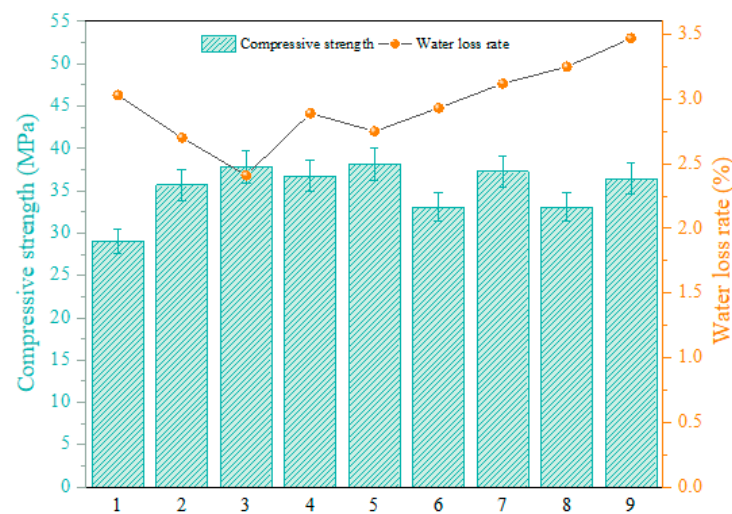**Figure 7.** The relationship between different VAE contents and 3 d water-loss rates of mortar.

Figure 8. The relationship between sodium silicate content and 7 d compressive strength of mortar.

3.2. Proportion of Composite Curing Agent Emulsion

In this experiment, the contents of VAE emulsions, film-forming additives (alcohol ester-12), and inorganic densification components (sodium silicate) were taken as test factors. The contents of VAE emulsions, alcohol ester-12, and sodium silicate were based on the quality of paraffin, and each factor was set to three levels (Figure 6). Table 6 shows the experimental design results of composites curing agents. The 3 d water-loss rate and 7 d compressive strength are shown in Figure 9.

Table 6. Experimental design of composite curing agent.

No.	VAE (%)	Alcohol Ester-12 (%)	Sodium Silicate (%)
1	A_1	B_1	C_1
2	A_1	B_2	C_2
3	A_1	B_3	C_3
4	A2	B2	C3
5	A2	B3	C1
6	A2	B1	C2
7	A3	B3	C2
8	A3	B1	C3
9	A3	B2	C1

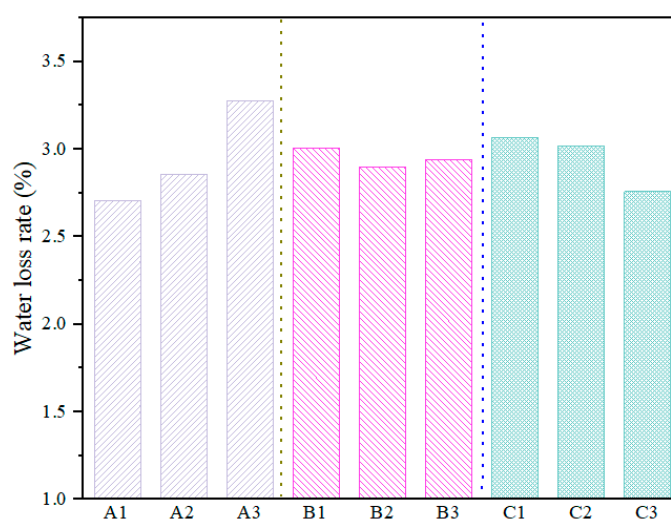**Figure 9.** Water-loss rate and compressive strength test results for different combinations.

The 3 d water-loss rate of the scheme 3 specimen reaches the lowest value in Figure 9, which is 3.67% lower than that of the uncoated curing agent. Additionally, the 3 d water-

loss rate value of the specimen under other dosages is also much lower than that of the uncoated curing agent specimen, while scheme 9 has the worst effect on the improvement of the water-retention performance of the specimen, which is reduced by 2.61% compared with the uncoated curing agent specimen. As shown in Table 7 and Figure 9, the strength of the curing agent CSB was generally higher than that of the control group. The compressive strength of scheme 3 is only 0.81% different from that of scheme 5.

Table 7. Orthogonal test factors and levels of curing agents.

Factors Level	A VAE (%)	B Alcohol Ester-12 (%)	C Sodium Silicate (%)
1	20	5	12
2	25	10	15
3	30	15	18

Further, the results in Figure 9 were analyzed as shown in Figures 10 and 11. It can be concluded from Figure 10 that the order of the factors affecting the water-loss rate of the specimen is A > C > B. The A_3 level increased by 0.42%, while the A_2 level increased by 0.15% compared with the A_1 level. It can be seen that the larger the proportion of VAE emulsion, the greater the water-loss rate of the specimen. The C_3 level is the lowest because the sodium silicate was involved in the cement hydration. Factor B had the least effect on the water-loss rate. Therefore, the optimal level combination of the best ratio of curing agent with water-loss rate as the evaluation index should be $A_1B_2C_3$. According to the analysis of Figure 11, the order of the factors affecting the compressive strength of the specimen is as follows: C > A > B. It was found that the optimal level combination of curing agent with strength should be $A_2B_2C_3$. The influence of sodium silicate on the strength of the specimen was obvious, and the influence of factor B was the least. However, for desert environments, the scheme with better water-retention performance was preferred, so the optimal combination was determined to be $A_1B_2C_3$ (20%VAE content, 10% alcohol ester-12 content, 18% sodium silicate content).

Figure 10. Trend chart of the relationship between factors and water-loss rate.
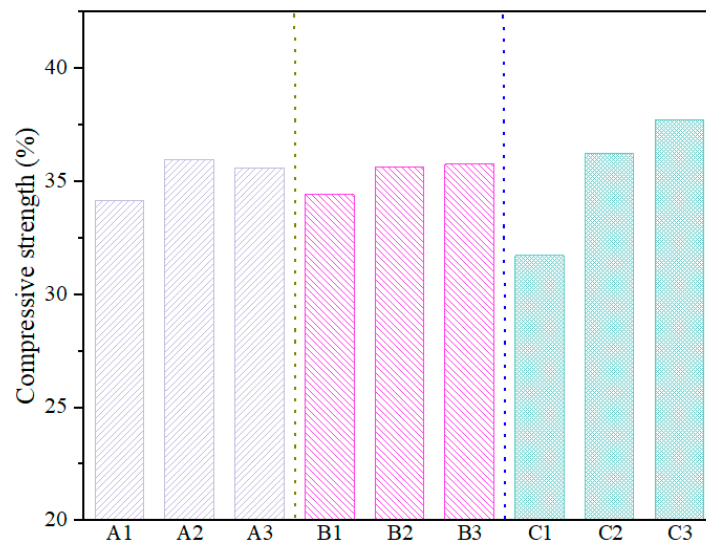
Figure 11. Trend chart of the relationship between factors and compressive strength.

3.3. Performance of Cement-Stabilized Base Coated with Curing Agent

3.3.1. Surface Morphology Characteristics of the Curing Agent in a Dry Environment

The surface morphology of the uncoated curing agent and the curing agent-coated specimen after curing in a dry environment is shown in Figure 12. Figure 12 shows different degrees of "whitening" [38–40] due to the formation of hydration products on the specimens. Compared with Figure 12c, there are more white substances on the surface of the test specimens in Figure 12d, which was due to the penetration of SiO_3^{2-} in sodium silicate into the surface of the specimen to promote cement hydration, resulting in more hydration products. In addition, the distribution of white substances is more uniform, which also indicates that the miscibility between the components of the composite curing agent was better after sodium silicate was mixed into the paraffin-VAE emulsion.

(**a**) Control group

(**b**) Paraffin film

(**c**) Paraffin-VAE film

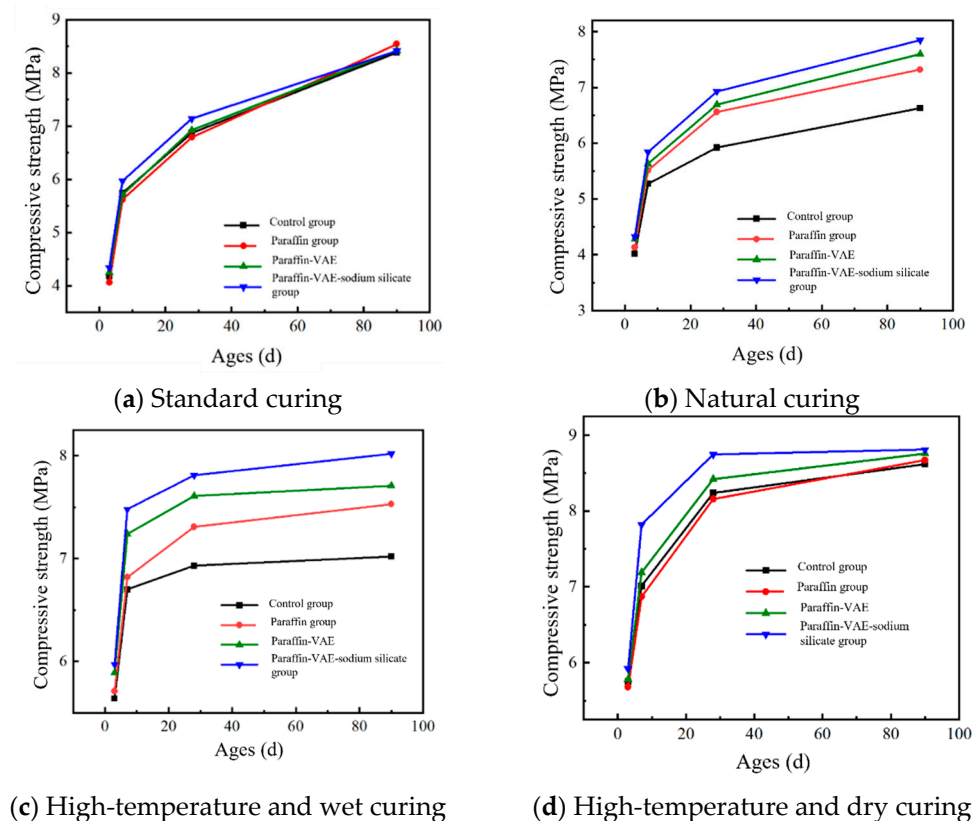(**d**) Paraffin-VAE-sodium silicate film
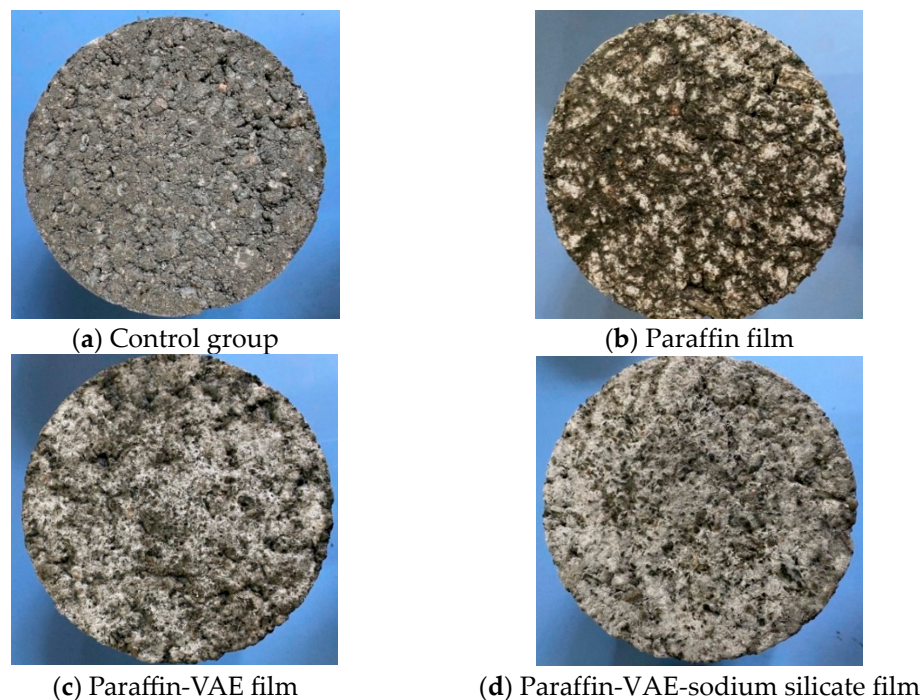
Figure 12. Surface topography of specimens without curing agent and with curing agent.

3.3.2. The Compressive Strength of Cement-Stabilized Base with Curing Agents

As Figure 13b shows, in the natural curing environment, there is little difference in the strength of all the groups at the 3 d and 7 d ages. At 28 d, the strength of the blank specimens increased by 12.3%, while that of the specimens coated with different curing agents increased by 19.0%, 18.8%, and 18.6% respectively. As reported in other research [41,42], the strength growth rate of the specimen coated with curing agent was larger than that without curing agent because of the water-retention effect of curing agents, so as to ensure that the cement-stabilized gravel mixture could complete hydration with its own water to the maximum extent and enhanced mechanical properties. In Figure 13d, it can be seen that the 7 d strength of the curing agent group and the control group is not much different due to the rapid cement hydration reaction at high temperature. The cement-stabilized base had high strength, but the strength growth of the curing agent group after 7 d was greater than that of the control group since the high temperature could accelerate the loss of free water. In the process of paraffin-VAE-sodium silicate curing cement-stabilizing gravel specimens, sodium silicate components penetrated into the surface of the specimens, participating in early hydration, and generated more hydration products. With the increase in age, sodium silicate had little influence on the compressive strength of cured specimens [43].

Comparing the four curing schemes, it can be seen that in desert environments and natural environments, the curing agent curing method can improve the strength of CSB because the curing agent can block the internal dispersion and loss of water to ensure the moisture required for cement hydration.

(**a**) Standard curing (**b**) Natural curing

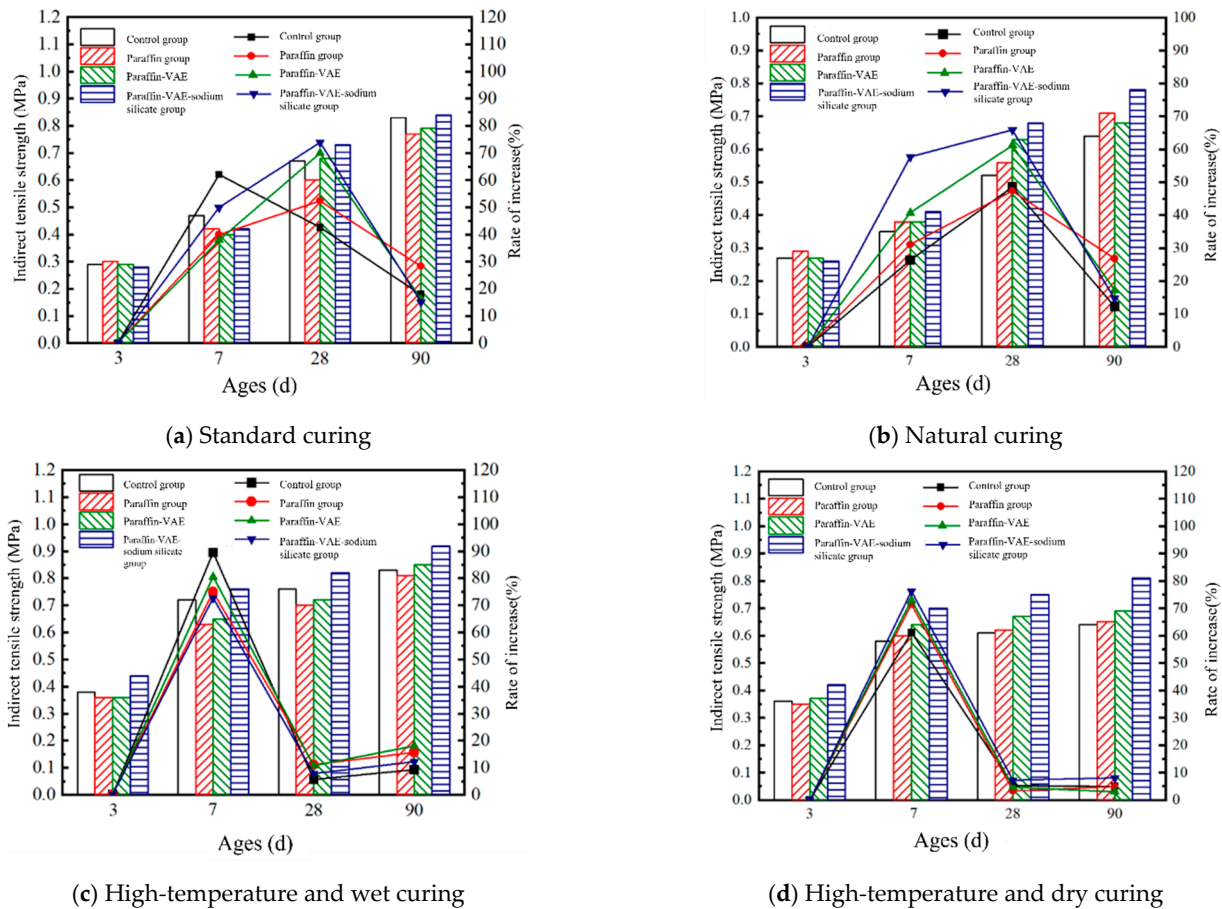(**c**) High-temperature and wet curing (**d**) High-temperature and dry curing

Figure 13. Compressive strength of cement-stabilized base at different ages with different curing conditions.

3.3.3. Indirect Tensile Strength of Cement-Stabilized Base

As shown in Figure 14, because the curing agent could block the entry of external moisture and reduce the cement hydration reaction rate, the 7 d strength growth of the

control group with standard curing and high-temperature wet curing is 62.1% and 89.5%, which is larger than that of the curing agent specimens. After 7 d, the growth of the control group was lower than others due to the destruction of the curing agent film, leading to an increase in internal humidity and acceleration of the cement hydration reaction. The 7 d indirect tensile strength growth rate of specimens coated with paraffin-VAE-sodium silicate curing agent was the largest because the sodium silicate component in the curing agent reacted with the Ca^{2+} in the cement, which increased the hydration products to block the pores. The 7 d indirect tensile strength of the CSB with the paraffin curing agent was higher than that with the paraffin-VAE curing agent specimen, indicating that the paraffin-VAE curing agent had a better water-retention effect than the paraffin curing agent.

(**a**) Standard curing

(**b**) Natural curing

(**c**) High-temperature and wet curing


(**d**) High-temperature and dry curing

Figure 14. The indirect tensile strength of cement-stabilized base.

In addition, curing humidity and temperature also had influence on the strength of the specimen, aligning with the findings of Mouret [44,45]. As the moisture inside the base could meet the normal hydration demand of cement, the hydration rate of cement is accelerated at high temperature, leading to a large number of hydration products being generated in a short time, promoting the early strength of the test specimen. It is found that the growth of 28 d splitting strength reaches the maximum under standard curing environments, while the growth rate of 7 d splitting strength reaches the maximum under high-temperature dry-curing environments. Aligning with the results of Hoy et al. [46], the humidity inside the curing agent group diffused and participated in the hydration, filling the pores with hydration products. As a result, a dense surface would prevent further loss and volatilization of water, so that the internal cement would continue to hydrate.

### 3.4. Durability of Cement-Stabilized Base with Composite Curing Agent

3.4.1. Dry Shrinkage Characteristics of Cement-Stabilized Base

As shown in Figure 15, the cumulative water-loss rate of the specimens with and without curing agent will gradually increase as time goes by. The cumulative water-loss rate without a curing agent reached 6.36% in 28 days, which indicated that the curing agent was significant to the curing process of the cement-stabilized base. The water-loss rate of the paraffin-VAE group was lower than that of the paraffin group, which proved that the incorporation of VAE emulsion could enhance the water-retention performance of the film. Compared with the paraffin-VAE specimens, the rate decreased after the addition of sodium silicate, because the inorganic component sodium silicate in the curing agent group participated in the early hydration reaction of cement and consumed a large amount of water.
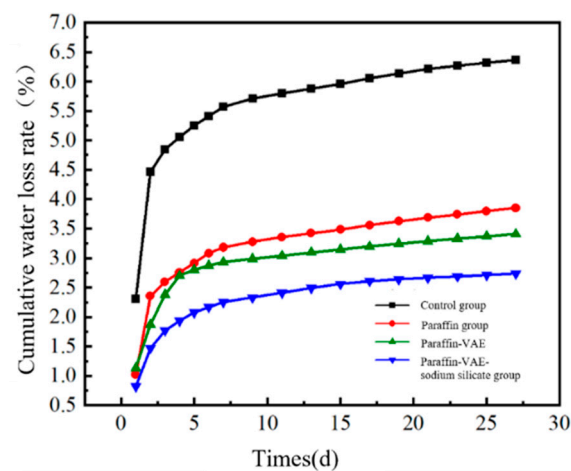
Figure 15. The relationship between the cumulative water-loss rate and time.

The dry shrinkage strain of the cement-stabilized base decreases with time in Figure 16. The value of the curing agent specimens is lower than that of the uncoated curing agent specimens, and the curing agent effectively reduced the risk of cracking. The cement hydration inside the base consumed a lot of water in the early stage and part of the water was lost, leading to an increase in the dry shrinkage. The curing agent blocked the free water, mitigating the internal water consumption. In the early stage of curing, the dry shrinkage strain decreased rapidly, while it tended to be stable after 7 d. Due to a large amount of capillary water decreasing in the early stage, the specimen lost too much water. Therefore, the dry shrinkage deformation mainly occurred in the early stage.
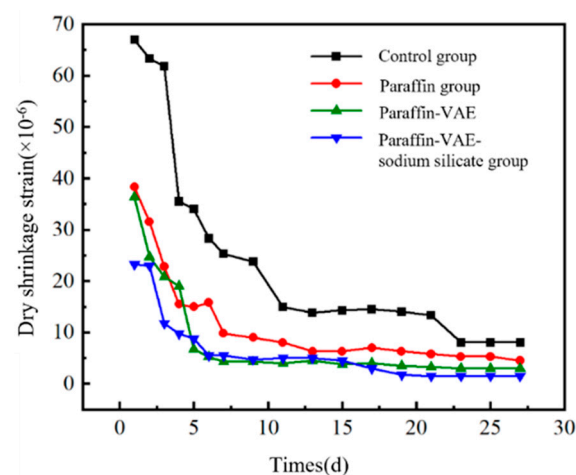
Figure 16. The relationship between the cumulative dry shrinkage strain and time.

3.4.2. Frost Resistance of the Cement-Stabilized Base

Due to the high temperature and humidity, after 28 d, most of the cement hydrated, so the cement-stabilized base had a relatively dense internal structure (Figure 17). Because of the evaporation of an amount of water in the early stage of curing, a part of the cement in the mixture was not completely hydrated. A part of the cement continued to hydrate in the melting stage of the wet freezing cycle, making the cement-stabilized gravel dense inside and increasing the compressive strength, which was confirmed in another study [47,48]. Under the conditions of dry and wet freezing, the strength of the samples with curing agents were greater than that of the control group, which indicated that the curing agent had a certain effect on the frost resistance of cement-stabilized bases. In addition, the compressive strengths of the paraffin-VAE-sodium silicate specimens are 7.48 MPa and 6.88 MPa, which were greater than those of the other two curing agent specimens. On the one hand, the sodium silicate participated in the cement hydration at an early stage and improved the compressive strength of the cement-stabilized base [49]. On the other hand, the hydration products made the surface dense, which could block the entry of water during the freeze–thaw cycle and reduce the damage caused by the freezing of internal moisture.
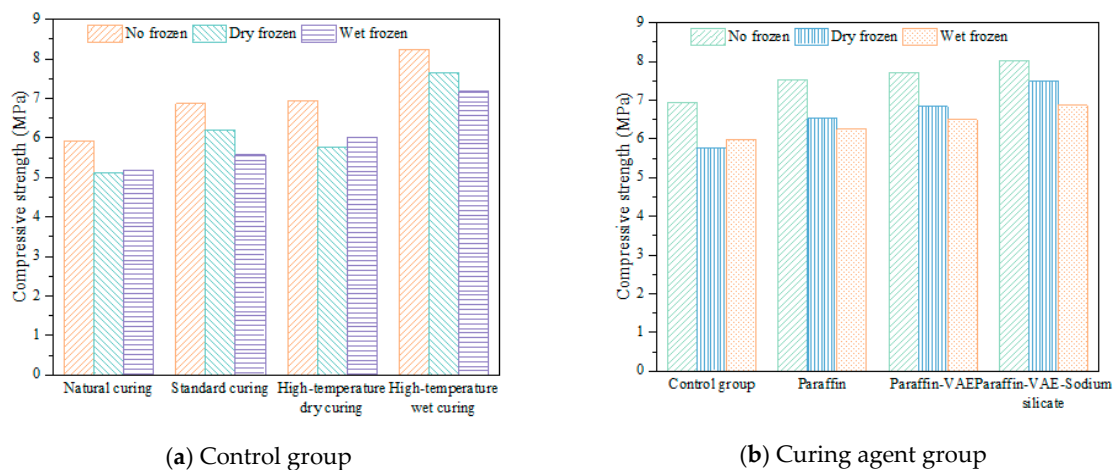
(**a**) Control group (**b**) Curing agent group

Figure 17. Compressive strength of the control group and curing agent group.

3.5. Microstructure of Cement-Stabilized Base Coated with Curing Agent

3.5.1. XRD Analysis

The XRD spectra of cement-hydration products cured via different curing agents under high-temperature and dry environments are shown in Figures 18 and 19. The main hydration products at 3 d and 7 d ages under different curing methods are CH and cement clinker. Due to the evaporation of the internal water and the loss of water in high-temperature dry culture environments, the hydration process was slow, and there was little $Ca(OH)_2$. In addition, the curing method of the curing agent was conducive to the formation of hydration products, so the C_2S peak value is lower. The curing agents could ensure hydration, promoting the density of the base structure and improving the strength and durability of the cement-stabilized base.
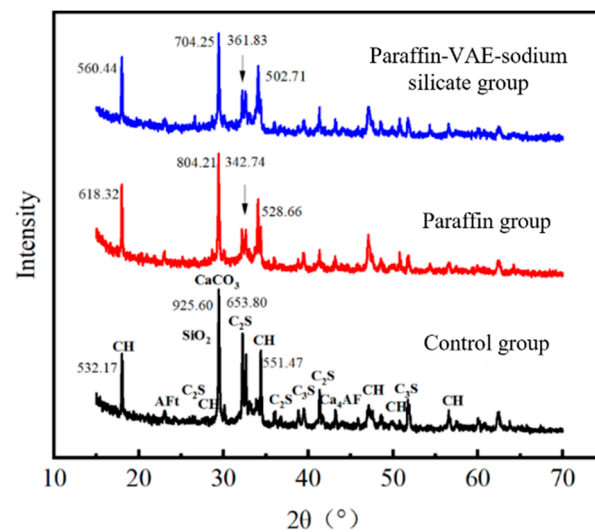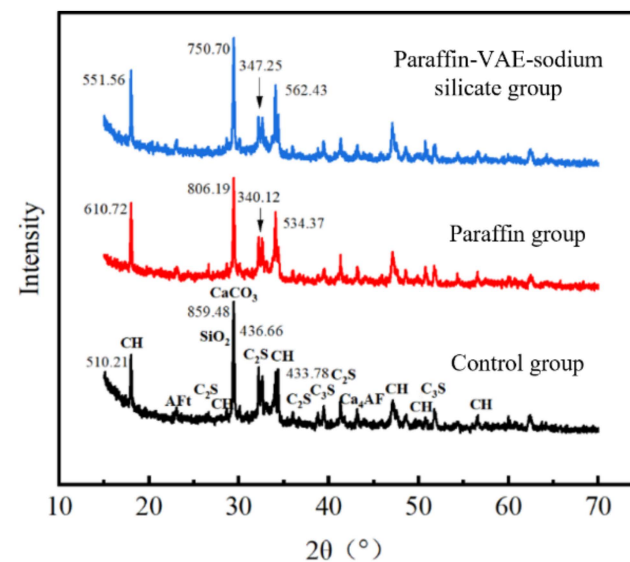
Figure 18. XRD diagram of 3 d hydration of cement.

Figure 19. XRD diagram of 7 d hydration of cement.

In the control group, CO_2 entered the specimen and reacted with $Ca(OH)_2$ to form calcium carbonate under the condition of high-temperature dry curing, and the cement specimen was carbonized, which hurt the mechanical properties and durability of the specimen. The curing agent could improve the carbonization resistance of the cement specimen.

3.5.2. TG Test

According to the DSC-TGA curves in Figure 20, the content of chemically bound water and CH in cement can be calculated via a formula, which is related to the degree of cement hydration [50,51], as shown in Table 8. The chemically bound water content of the 3 d paraffin-VAE-sodium silicate group was 1.744% and 5.788% higher than that of the paraffin and control group. At the same time, the CH content of the paraffin-VAE-sodium silicate group was the highest under different curing methods, which indicated that the number of hydration products such as C-S-H, AFt, and CH was the largest in the paraffin-VAE-sodium silicate group. Thus, the curing agent had a significant effect on the hydration degree of cement, which was helpful with respect to the mechanical properties and durability.

Also, during the 3 d–7 d age period, the chemically bound water of the control group, paraffin group, and paraffin-VAE-sodium silicate group increased by 3.519%, 2.768%, and 2.217%, respectively. The chemically bound water of the blank group increased the most, and the CH content of control group increased by 5.181%, while the paraffin group and paraffin-VAE-sodium silicate group increased by 3.135% and 2.775%. The increased amount is lower than that of the control group, and it was reported that [52] during the 7 days, cement hydration generates a large number of hydration products to fill the pores, and the hydration products are wrapped on the surface of the cement clinker, which delays the chemical reaction between the cement and free water [53].
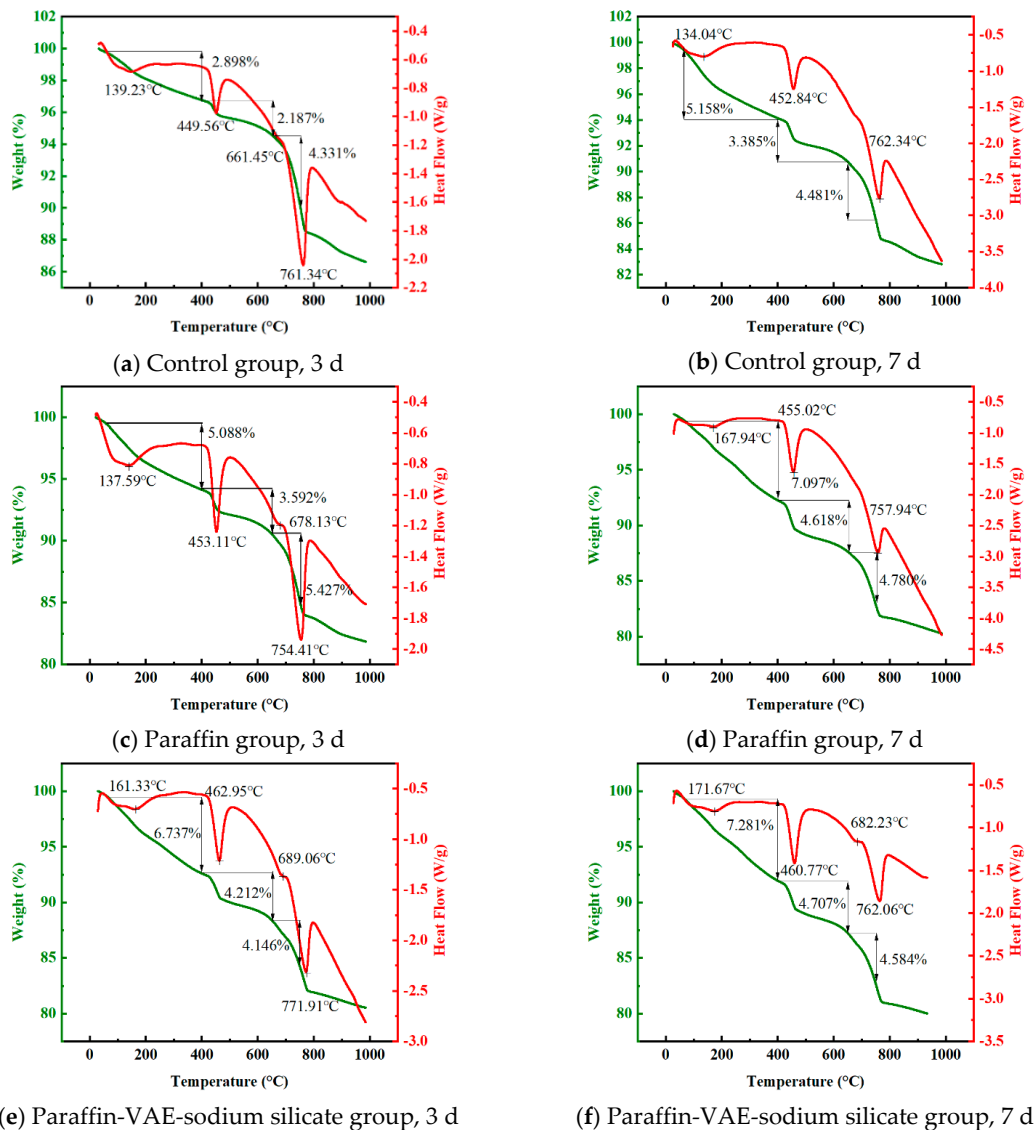

(**a**) Control group, 3 d

(**b**) Control group, 7 d

(**c**) Paraffin group, 3 d

(**d**) Paraffin group, 7 d

(**e**) Paraffin-VAE-sodium silicate group, 3 d

(**f**) Paraffin-VAE-sodium silicate group, 7 d

**Figure 20.** DSC–TGA curves of cement hydration with different curing agents.

Table 8. The contents of chemically bound water and CH in cement hydration products.

Age	Type	Control Group	Paraffin Group	Paraffin-VAE-Sodium Silicate Group
3 d	Chemically bound water (%)	6.857	10.901	12.645
	Ca(OH)$_2$ (%)	16.298	23.927	24.322
7 d	Chemically bound water (%)	10.376	13.669	14.862
	Ca(OH)$_2$ (%)	21.479	27.062	27.097

3.5.3. Microscopic Topography Observation with SEM

(1)　Microscopic morphology of curing agent films

There are a large number of strips on the surface of the paraffin film in Figure 21, and the strip structures are of different lengths and are darker around the strips. After the loss of water in the emulsion, the paraffin emulsion breaks the emulsion, and the paraffin particles gather, but the aggregation between the particles is weak, resulting in the thickness of this part being thin and susceptible to external erosion damage, resulting in poor sealing, which harms the curing effect of cement-stabilized gravel specimens. Therefore, paraffin alone could not ensure the curing effect of the base. After being mixed with VAE emulsion, the surface brightness of the paraffin-VAE film is brighter, indicating that the surface of the film is dense, but there are still some pores and water migration is lost from the pores, which reduces the water-retention performance of the film. Compared with the paraffin-VAE film, the inorganic sodium silicate incorporation leads to a reduction in the porosity of the film, the surface being brighter, the film being denser, and the water-retention performance being better, which is conducive to the curing effect of the curing agent. This is consistent with previous research results; the interaction between the three components and their respective properties together improved the curing effect and significantly reduced the internal water consumption.
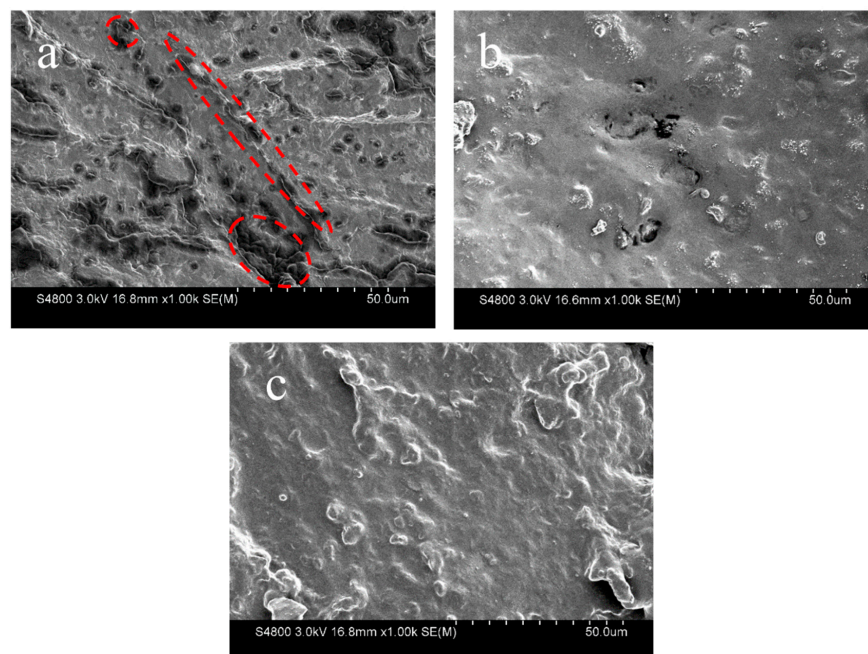
Figure 21. Surface topography of different curing agent films. (**a**) Paraffin film morphology; (**b**) Morphology of paraffin-VAE film; (**c**) Morphology of paraffin-VAE-sodium silicate film.
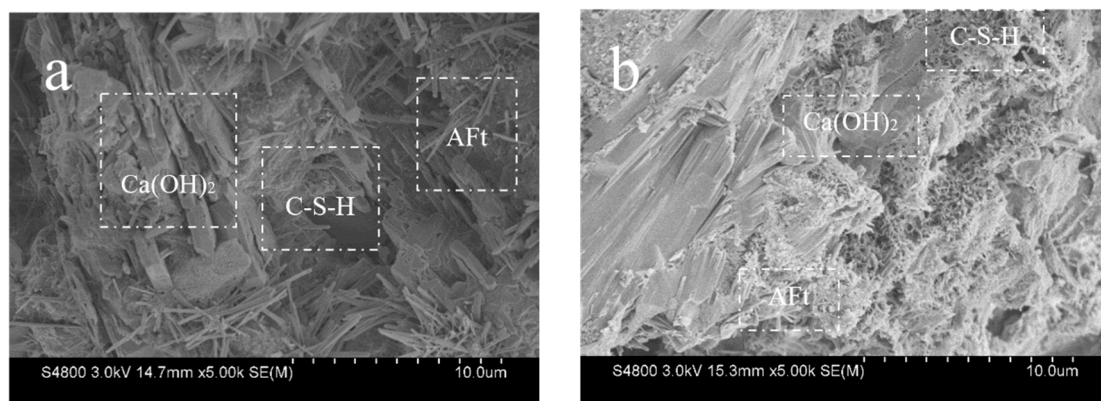
(2)　Topography of cement-stabilized base with different curing agents

Figure 22a shows that during the 3-day aging of the paraffin curing agent specimen, the convex destroys the paraffin film, and the hydration products continue to grow through the film. A number of hydration products appeared in the damaged area of the paraffin film and the hydration products filled the pores of the film so that the surface of the specimen was dense, which could preserve the water-retaining effect. In Figure 22b, during the 3-day aging of the paraffin-VAE-sodium silicate curing agent specimen, a large number of aluminites and C-S-H gels were generated.
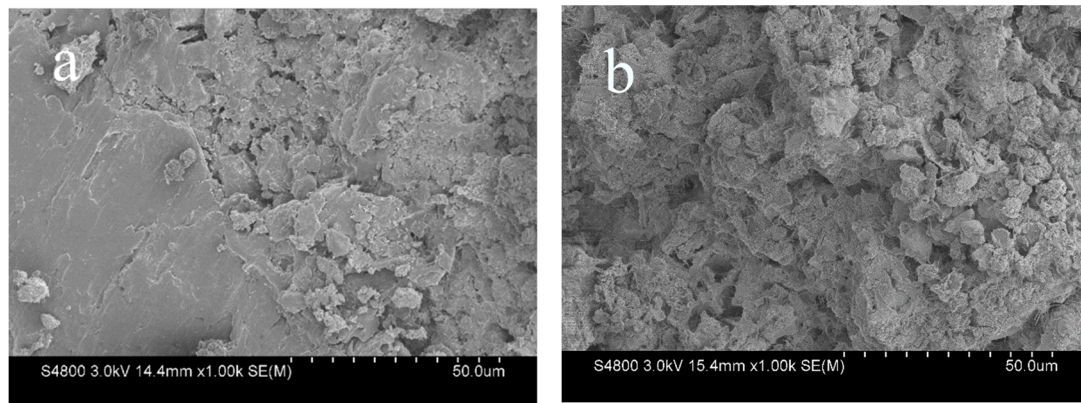
Figure 22. Surface morphology of base with different curing agents at 7 d. (**a**) Paraffin curing specimen morphology; (**b**) Morphology of paraffin-VAE-sodium silicate curing specimen.

There is a large number of pores in the uncoated curing agent specimen in the high-temperature dry-curing environment (Figure 23), and the inside of the coated curing agent specimen is denser than that of the non-coated curing agent specimen. The C-S-H and CH in the specimen with curing agent are connected to make the cement structure stable. The morphology of the specimen without the curing agent is porous and loose. In addition, there is a large number of fine needle-like alum in the hydration products, while the cement-hydration products inside the curing agent specimens have large crystalline grains, which are cross-connected with C-S-H and CH. Due to the presence of a curing agent, the cement could fully hydrate, which was conducive to an improvement in the strength and durability of the cement stable base. The compactness of the curing agent specimens was higher than that of the non-curing agent specimens, and the curing agent had a better curing effect on the specimens in the high-temperature dry-curing environment.

Figure 23. Internal morphology of cement-stabilized base with/without curing agent. (**a**) Morphology of specimen with curing agent; (**b**) Morphology of specimen without curing agent.

4. Conclusions

In this paper, the curing agent was used to maintain the cement-stabilized base material in the desert environment. The strength performance and durability of cement-stabilized bases in desert environments were studied. Finally, the mechanism of the curing agent on cement was explored. The following are the main conclusions:

(1) Taking the water-loss rate and compressive strength as the evaluation indexes, the optimal ratio of the curing agent components was finally determined, and the quality of the paraffin emulsion was taken as the benchmark. The content of VAE emulsion was 20%, the content of alcohol ester-12 was 10%, and the content of sodium silicate was 18%.

(2) The curing agent could effectively promote the performance of cement-stabilized bases. In a high-temperature and dry environment, the composite curing agent effectively protected the moisture from loss, so that the compressive strength of the cement base was significantly improved. The inorganic sodium silicate SiO_3^{2-} participated in the cement hydration, and the hydration products filled the voids to prevent further water loss, which was conducive to the development of strength in the later stage.

(3) The curing agent affected the frost resistance. The paraffin-VAE-sodium silicate curing agent curing method could alleviate the drying shrinkage of the specimen, reduce the cracks in the pavement, and improve the durability of the pavement.

(4) The incorporation of sodium silicate accelerated the early hydration of cement on the surface, leading to an increase in CH content. After the paraffin emulsion was incorporated with VAE emulsion and sodium silicate, the porosity of the film was reduced and the water-retention performance was improved. Because the grain of the cement-hydration products of the curing agent group increased, the cross-connection made the surface of the cement stone more compact.

This study mainly focuses on the external curing of cement-stabilized bases. In the future, paying more attention to the research about different types of semi-rigid bases and seeking different types of curing agents and methods are significant and necessary. In addition, curing of semi-rigid bases in different extreme environments will always be an issue, so proposing appropriate curing methods for different environments is also worthy of attention.

Author Contributions: Conceptualization, C.W.; Methodology, J.M.; Formal analysis, Z.H., Y.S. and Q.Y.; Investigation, C.W. and M.L.; Writing—original draft, X.S.; Writing—review & editing, Z.H.; Supervision, M.L. All authors have read and agreed to the published version of the manuscript.

Data Availability Statement: Data will be made available on request.

Conflicts of Interest: Authors Chenhao Wei, Jiachen Ma, Yana Shi, Qiang Yi and Maoqing Li were employed by the company Shaanxi Coal Chemical Industry Technology Research Institute Co., Ltd. Author Xiaohui Sun was employed by the company CCCC SHEC Construction Technology Branch Company. The remaining author declare that the research was conducted in the absence of any commercial or financial relationships that could be construed as a potential conflict of interest.

References

1. Li, X.; Ran, W. Dynamic response analysis of semi-rigid base asphalt pavement considering interlayer contact state and cracks. *J. Shihezi Univ. (Nat. Sci. Ed.)* **2020**, *38*, 586–592.
2. Sha, A. Material Properties of Semi-rigid Base Layer. *China J. Highw. Transp.* **2008**, *21*, 1–5.
3. He, H.; Shuang, E.; Lu, D.; Hu, Y.; Yan, C.; Shan, H.; He, C. Deciphering size-induced influence of carbon dots on mechanical performance of cement composites. *Constr. Build. Mater.* **2024**, *425*, 136030. [CrossRef]
4. Zheng, Y.; Zhang, P.; Cai, Y.; Jin, Z.; Moshtagh, E. Cracking resistance and mechanical properties of basalt fibers reinforced cement-stabilized macadam. *Compos. Part B* **2019**, *165*, 312–334. [CrossRef]
5. Zhao, C.; Liang, N.; Zhu, X.; Yuan, L.; Zhou, B. Fiber-reinforced cement-stabilized Macadam with Various Polyvinyl Alcohol Fiber Contents and Lengths. *J. Mater. Civ. Eng.* **2020**, *32*, 04020312. [CrossRef]
6. Du, S. Mechanical properties and shrinkage characteristics of cement stabilized macadam with asphalt emulsion. *Constr. Build. Mater.* **2019**, *203*, 408–416. [CrossRef]
7. Sun, X.; Wu, S.; Yang, J.; Yang, R. Mechanical properties and crack resistance of crumb rubber modified cement-stabilized macadam. *Constr. Build. Mater.* **2020**, *259*, 119708. [CrossRef]
8. Liu, Z. Experimental Research on the Engineering Characteristics of Polyester Fiber–Reinforced Cement-Stabilized Macadam. *J. Mater. Civ. Eng.* **2015**, *27*, 04015004. [CrossRef]
9. Olgun, M. Effects of polypropylene fiber inclusion on the strength and volume change characteristics of cement-fly ash stabilized clay soil. *Geosynth. Int.* **2013**, *20*, 263–275. [CrossRef]
10. Nhieu, D.V.; Hoy, M.; Horpibulsuk, S.; Karntatam, K.; Arulrajah, A.; Horpibulsuk, J. Cement–natural rubber latex stabilised recycled concrete aggregate as a pavement base material. *Road Mater. Pavement Des.* **2023**, *24*, 1636–1650. [CrossRef]

11. Hoy, M.; Nhieu, D.V.; Suddeepong, A.; Horpibulsuk, S.; Arulrajah, A.; Deng, Y.; Udomchai, A. Stiffness, rutting, and fatigue performance evaluation of cement-natural rubber latex stabilized recycled concrete aggregate. *Int. J. Pavement Eng.* **2023**, *24*, 2276204. [CrossRef]

12. Tran, N.Q.; Hoy, M.; Suddeepong, A.; Horpibulsuk, S.; Kantathum, K.; Arulrajah, A. Improved mechanical and microstructure of cement-stabilized lateritic soil using recycled materials replacement and natural rubber latex for pavement applications. *Constr. Build. Mater.* **2022**, *347*, 128547. [CrossRef]

13. Udomchai, A.; Buritatum, A.; Suddeepong, A.; Hoy, M.; Horpibulsuk, S.; Arulrajah, A.; Horpibulsuk, J. Evaluation of durability against wetting and drying cycles of cement-natural rubber latex stabilised unpaved road under cyclic tensile loading. *Int. J. Pavement Eng.* **2022**, *23*, 4442–4453. [CrossRef]

14. Deng, C.; Jiang, Y.; Lin, H.; Ji, X. Mechanical-strength-growth law and predictive model for cement-stabilized macadam. *Constr. Build. Mater.* **2019**, *215*, 582–594. [CrossRef]

15. Tran, T.T.; Nguyen, T.; Pham, P.N.; Nguyen, H.H.; Nguyen, P.Q. Thermal distribution in cement-treated base: Effect of curing methods and temperature estimation using Artificial Neural Networks. *Constr. Build. Mater.* **2021**, *279*, 122528. [CrossRef]

16. He, X.; Yang, Q.; He, G. Erosion resistance of polypropylene fiber reinforced cement stabilized gravel base material. *J. Build. Mater.* **2010**, *13*, 263–267+276.

17. He, X.; Yang, Q.; Yi, Z. Research on erosion resistance test evaluation method of cement stabilized macadamia base material. *J. Chongqing Jiaotong Univ. (Nat. Sci. Ed.)* **2009**, *28*, 555–558+564.

18. Mao, X.; Li, W.; Wang, T.; Zhang, H.; Wang, L.; Zhang, H. Study on health preserving mode of new semi-rigid materials in high cold area. *Road Build. Mach. Constr. Mech.* **2016**, *33*, 49–52.

19. Xie, Q.; Chen, X.; Wen, L. Development status and prospect of concrete curing agent. *Bull. Silic.* **2016**, *35*, 1761–1766+1771.

20. Al-Gahtani, A.S. Effect of curing methods on the properties of plain and blended cement concretes. *Constr. Build. Mater.* **2010**, *24*, 308–314. [CrossRef]

21. Kalinowski, M.; Woyciechowski, P.; Sokolowska, J. Effect of mechanically-induced fragmentation of polyacrylic superabsorbent polymer (SAP) hydrogel on the properties of cement composites. *Constr. Build. Mater.* **2020**, *263*, 120135. [CrossRef]

22. Snoeck, D.; Moerkerke, B.; Mignon, A.; De Belie, N. In-situ crosslinking of superabsorbent polymers as external curing layer compared to internal curing to mitigate plastic shrinkage. *Constr. Build. Mater.* **2020**, *262*, 120819. [CrossRef]

23. Lura, P.; Wyrzykowski, M.; Tang, C.; Lehmann, E. Internal curing with lightweight aggregate produced from biomass-derived waste. *Cem. Concr. Res.* **2014**, *59*, 24–33. [CrossRef]

24. Ghourchian, S.; Wyrzykowski, M.; Lura, P.; Shekarchi, M.; Ahmadi, B. An investigation on the use of zeolite aggregates for internal curing of concrete. *Constr. Build. Mater.* **2013**, *40*, 135–144. [CrossRef]

25. Ma, X.; Liu, J.; Shi, C. A review on the use of LWA as an internal curing agent of high performance cement-based materials. *Constr. Build. Mater.* **2019**, *218*, 385–393. [CrossRef]

26. Xue, B.; Pei, J.; Sheng, Y.; Li, R. Effect of curing compounds on the properties and microstructure of cement concretes. *Constr. Build. Mater.* **2015**, *101*, 410–416. [CrossRef]

27. Sun, Y.; Li, L. Strength assessment and mechanism analysis of cement stabilized reclaimed lime-fly ash macadam. *Constr. Build. Mater.* **2018**, *166*, 118–129. [CrossRef]

28. Yan, K.; Sun, H.; Gao, F.; Ge, D.; You, L. Assessment and mechanism analysis of municipal solid waste incineration bottom ash as aggregate in cement stabilized macadam. *J. Clean. Prod.* **2020**, *244*, 118750. [CrossRef]

29. Li, X.; Lv, X.; Wang, W.; Liu, J.; Yu, M.; You, Z. Crack resistance of waste cooking oil modified cement stabilized macadam. *J. Clean. Prod.* **2020**, *243*, 118525. [CrossRef]

30. Castro, J.; Keiser, L.; Golias, M.; Weiss, J. Absorption and desorption properties offine lightweight aggregate for application to internally cured concrete mixtures. *Cem. Concr. Compos.* **2011**, *33*, 1001–1008. [CrossRef]

31. Song, C. Study on Temperature Field of Roadbed and Pavement Working Environment Temperature Index in Desert Area. Ph.D. Thesis, Chang'an University, Xi'an, China, 2006.

32. Li, J.; Wang, X.; Wang, Y. Study on typical pavement structure in desert area. *Highway* **2006**, *11*, 39–43.

33. Li, A.; Yang, H.; Hao, P. Study on health preservation technology of cement stabilized soil pavement in desert highway. *Road Constr. Mach. Constr. Mech.* **2005**, *22*, 41–44.

34. Li, M.; Liu, J.; Tian, Q.; Wang, W.; Wang, W. Early-age deformation behavior of cement-based materials under internal curing. *J. Chin. Ceram.* **2017**, *45*, 1635–1641.

35. *GB175-2007*; Common Portland Cement. National Standard of the People's. Republic of China: Beijing, China, 2007.

36. *JTGE30-2005*; Test Methods of Cement and Concrete for Highway Engineering. National Standard of the People's. Republic of China: Beijing, China, 2005.

37. *JTG E51-2009*; Test Methods of Materials Stabilized with Inorganic Binders for Highway Engineering. National Standard of the People's. Republic of China: Beijing, China, 2009.

38. Wang, Y.; Geng, Y.; Zhang, H.; Wang, J.; Yuan, L. Effect of nano-silica on alkali-activated slag cement efflorescence. *Bull. Chin. Ceram. Soc.* **2020**, *39*, 1451–1456+1465. [CrossRef]

39. Yan, F.; Jin, Q.; Lou, Z. Research on treatment of efflorescence of concrete products. *China Build. Mater. Sci. Technol.* **2020**, *29*, 68–69+87.

40. Xue, L.; Li, H.; Gao, Y. Analysis of the reasons for efflorescence performance of decorative mortar based on aluminate cement and gypsum system. *Bull. Chin. Ceram. Soc.* **2018**, *37*, 3213–3216+3222.
41. Sampebulu, V. Increase on strengths of hot weather concrete by self-curing of wet porous aggregate. *Civ. Eng. Dimens.* **2012**, *14*, 92–99. [CrossRef]
42. Rizzuto, J.P.; Kamal, M.; Elsayad, H.; Bashandy, A.; Etman, Z.; Roos, M.N.A.; Shaaban, I.G. Effect of self-curing admixture on concrete properties in hot climate conditions. *Constr. Build. Mater.* **2020**, *261*, 119933. [CrossRef]
43. Liu, Y.; Wang, B.; Fan, Y.; Yu, J.; Shi, T.; Zhou, Y.; Song, Y.; Xu, G.; Xiong, C.; Zhou, X. Effects of reactive MgO on durability and microstructure of cement-based materials: Considering carbonation and pH value. *Constr. Build. Mater.* **2024**, *426*, 136216. [CrossRef]
44. Benouadah, A.; Nabil, B.; Benammar, A. Effect of Self-Curing Admixture and Sand Type on the Mechanical and Microstructural Properties of Concrete in Hot Climate Conditions. *Ann. De Chim. Sci. Des Matériaux* **2024**, *48*, 85–93. [CrossRef]
45. Mouret, M.; Bascoul, A.; Escadeillas, G. Drops in concrete strength in summer related to the aggregate temperature. *Cem. Concr. Res.* **1997**, *27*, 345–357. [CrossRef]
46. Hoy, M.; Nhieu, D.V.; Horpibulsuk, S.; Suddeepong, A.; Chinkulkijniwat, A.; Buritatum, A.; Arulrajah, A. Effect of wetting and drying cycles on mechanical strength of cement-natural rubber latex stabilized recycled concrete aggregate. *Constr. Build. Mater.* **2023**, *394*, 132301. [CrossRef]
47. Hoy, M.; Tran, N.Q.; Suddeepong, A.; Horpibulsuk, S.; Buritatum, A.; Yaowarat, T.; Arulrajah, A. Wetting-drying durability performance of cement-stabilized recycled materials and lateritic soil using natural rubber latex. *Constr. Build. Mater.* **2023**, *403*, 133108. [CrossRef]
48. He, H.; Qiao, H.; Sun, T.; Yang, H.; He, C. Research progress in mechanisms, influence factors and improvement routes of chloride binding for cement composites. *J. Build. Eng.* **2024**, *86*, 108978. [CrossRef]
49. Ma, S.; Gao, J.; Wei, J.; Zhang, X. Study on unconfined compressive and frost resistance of low temperature early strength cement stabilized macadam material. *Bull. Chin. Ceram. Soc.* **2019**, *38*, 756–761.
50. Zhou, S.; Huang, X.; Liang, X.; Zhao, P. Analysis of the hydration process of slag in the cement using DSC-TG method. *Mater. Rep.* **2012**, *26*, 358–360+377.
51. Yan, L.; Zhou, W.; You, Q.; Jiang, Y.; Wu, D. Semi quantifying ettringite by DSC-TG. *New Build. Mater.* **2015**, *42*, 41–43.
52. Qin, X.; Shen, A.; Lyu, Z.; Shi, L.; Yang, J.; Liu, H. Research on water transport behaviors and hydration characteristics of internal curing pavement concrete. *Constr. Build. Mater.* **2020**, *248*, 118714. [CrossRef]
53. Zeng, H.; Jin, M.; Li, W.; Gao, C.; Ma, Y.; Guan, Q.; Liu, J. Performance evolution of low heat cement under thermal cycling fatigue: A comparative study with moderate heat cement and ordinary Portland cement. *Constr. Build. Mater.* **2024**, *412*, 134863. [CrossRef]